Dynamic fabric modelling and simulation using deformable models

Article *in* The Journal of The Textile Institute · August 2011

DOI: 10.1080/00405000.2010.514724

3 authors:

Hassen Hedfi
University of Monastir
7 PUBLICATIONS **29** CITATIONS
SEE PROFILE

Adel Ghith
Ecole Nationale d'Ingénieurs de Monastir
7 PUBLICATIONS **64** CITATIONS
SEE PROFILE

Hédi Belhadjsalah
University of Monastir-Ecole Nationale d'Ingénieurs de Monastir
133 PUBLICATIONS **1,368** CITATIONS
SEE PROFILE

Journal of the Textile Institute
Publication details, including instructions for authors and subscription information:
http://www.informaworld.com/smpp/title~content=t778164490

Dynamic fabric modelling and simulation using deformable models

Hassen Hedfi[a]; Adel Ghith[b]; Hédi BelHadjSalah[a]
[a] Mechanical Engineering Laboratory, National Engineering School of Monastir, Monastir 5019, Tunisia [b] Thermal and Energetic Systems Studies Laboratory, National Engineering School of Monastir, Monastir 5019, Tunisia

First published on: 18 February 2011

To cite this Article Hedfi, Hassen , Ghith, Adel and BelHadjSalah, Hédi(2011) 'Dynamic fabric modelling and simulation using deformable models', Journal of the Textile Institute, 102: 8, 647 — 667, First published on: 18 February 2011 (iFirst)
To link to this Article: DOI: 10.1080/00405000.2010.514724
URL: http://dx.doi.org/10.1080/00405000.2010.514724

The Journal of The Textile Institute
Vol. 102, No. 8, August 2011, 647–667

Taylor & Francis
Taylor & Francis Group

Dynamic fabric modelling and simulation using deformable models

Hassen Hedfi[a]*, Adel Ghith[b] and Hédi BelHadjSalah[a]

[a]*Mechanical Engineering Laboratory, National Engineering School of Monastir, Monastir 5019, Tunisia;*
[b]*Thermal and Energetic Systems Studies Laboratory, National Engineering School of Monastir, Monastir 5019, Tunisia*

(*Received 13 January 2010; final version received 4 August 2010*)

This paper proposes a modelling of the dynamic behaviour of textile fabrics based on a new formulation of deformable models. Deformable models such as those that were introduced by Terzopoulos in 1987 for modelling and simulation of deformable objects in computer graphics are reformulated to simulate textile woven fabrics. This investigation tends to produce simulations of textile fabrics showing the dynamic aspect of their behaviour while remaining faithful to the physical reality of material. The developed model takes into account several mechanical and physical parameters of textile fabrics. Numerical resolution of partial differential equations controlling the behaviour of textile fabrics is made by using the finite element method. Several simulations are carried out and compared with the experimental results. A drape-meter test is simulated and the results are strongly correlated with those obtained in experiments.

Keywords: woven fabric; deformable models; dynamic behaviour; finite element method

Introduction

Textile structures modelling and simulation represent a field of research under increasing development. Industrial applications of this scientific research activity are numerous: computer-aided design of clothing (Fontana, Carubelli, Rizzi, & Cugini, 2005; Fontana, Rizzi, & Cugini, 2004; Volino, Cordier, & Magnenat-Thalmann, 2005), virtual prototyping (Charlie & Kai, 2008; Kim & Kang, 2002; Luo & Yuen, 2005; Volino & Magnenat-Thalmann, 2005) and virtual trade (Bingham et al., 2007; Cordier, Seo, & Magnenat-Thalmann, 2003; Liang, Jinlian, & Baciu, 2006). Nevertheless, in applications related to computer animation (Oh, Noh, & Wohn, 2008), cinematography (Carignan, Yang, Magnenat-Thalmann, & Thalmann, 1992), and video games industry (Müller, Heidelberger, Hennix, & Ratcliff, 2007), the modelling and the simulation of fabrics and textile clothing are frequently used. In textile fabrics modelling and simulation, two scientific communities are mainly distinguished: researchers in textiles and those in computer graphics. For computer graphics researchers, the objective is to reproduce simulations of the textile material in the most realistic way without being necessarily faithful to the physical reality of the simulated object. However, for researchers in textiles, the objective is to develop a model which takes into account the mechanical and physical properties of the textile material. Accordingly, tools and methods developed and used by each community are in general different. In this context, two types of textile fabrics modelling are distinguished: particles-based models and continuum models. The first are massively used in computer graphics (Baraff & Witkin, 1998; Breen, House, & Getto, 1992; Breen, House, & Wozny, 1994; Eberhardt, Olaf, & Michael, 2000; In, Tae, Sung, & Chi, 2006; Provot, 1995). However, continuum models are in general developed and used by researchers in textiles and mechanics. Many studies have been developed using shell formulation (Chen & Govindaraj, 1995; Garg, Grinspun, Wardetzky, & Zorin, 2007; Jeffrey, Shigan, & Timothy, 1996; Liu & Sze, 2009; Stylios, Wan, & Powell, 1996), beam formulaion (Ascough, Bez, & Bricis, 1996), thin-plate concept (Chen, Sun, & Yuen, 1998), cosserat surface (Wu & de Melo, 2004) and finite element formulations (Behera, Pattanayak, & Mishra, 2008; Collier, Collier, O'Toole, & Sarg, 1991; Kang & Yu, 1995). For dynamic drape modelling and simulation, we mention the work of Yu, Kang, and Chung (2000), in which the authors presented an explicit algorithm for the finite element method (FEM) resolution of a dynamic model based on shell theory. The objective was the simulation of fabrics drape behaviour. The developed model took into account the inertial, internal and external efforts undergone by the fabric. The authors also treated the

*Corresponding author. Email: hassen_hedfi@yahoo.com

ISSN 0040-5000 print/ISSN 1754-2340 online

DOI: 10.1080/00405000.2010.514724
http://www.informaworld.com

effects of viscous damping and proposed an algorithm for contact treatment. The validation of the numerical model was made by simulating fabrics draped on tables and virtual clothed mannequin. Yu, Zampaloni, Pourboghrat, Chung, and Kang (2005) were interested in the flexible bending behaviour of woven reinforcements. A detailed numerical study was carried out showing the effect of the shearing and the asymmetry factor. Simulations of composite stamping were presented and compared with the experiments. Although this work is focused on woven reinforcements, it remains nevertheless of great utility in simulation of fabrics for apparel applications.

We mention some papers in which the reader may find more detailed reviews concerning various methods of textile fabrics modelling and simulations. Hauth et al. (2002) presented a comparative study between discrete modelling (particles- or mass-springs-based models) and continuum-based formulations (plate, shell, or deformable models formulations). In some other papers (Bridson, Fedkiw, & John, 2002; Hauth, Etzmuß, & Straßer, 2003; Volino & Magnenat-Thalmann, 2001; Zink & Hardy, 2007), comparative studies between different methods of resolution of the equations controlling the textile materials' behaviour were introduced. Techniques used for resolution and treatment of collisions and self-collisions problems were also discussed. Magnenat-Thalmann, Volino, and Cordier (2002) discussed the avenue of research in dynamic clothing, and Choi and Ko (2005) presented and argued various problems and challenges to overcome in the fabrics modelling and simulation.

Deformable models are classified among the continuum models. They were introduced by Terzopoulos in 1987 for deformable objects modelling and simulation. Terzopoulos, Platt, Barr, and Fleischer (1987) exposed the concept of deformable objects and proposed a model based on differential geometry and analytical mechanics, unifying the description of shape and motion of an object throughout time. This formulation can be used for modelling and simulation of 1D, 2D and 3D objects produced from deformable materials. The author used the finite difference method to solve numerically the partial differential equations (PDE) controlling the model. The presented results seem to be persuading. However, to control the object deformations, Terzopoulos introduced some coefficients detached of any physical significance. Terzopoulos and Fleischer (1988a) developed other aspects of deformable objects behaviour by introducing the cases of viscoelastic and plastic behaviour and the rupture of deformable object. Terzopoulos and Fleischer (1988b) and Terzopoulos and Witkin (1988) proposed to subdivide motion of the object into two components: rigid body and deformable body motion. In all these papers, the authors omitted the details leading to their formulations. As for the presented results, the authors indicated neither the imposed boundary conditions nor the computing performances.

De Santa, Wu, and Costa (1997) studied the use of some concepts from differential geometry to control the manipulation of the deformable model proposed by Terzopoulos. The authors were particularly interested in the animation of deformable panels without stretching (area invariant), such as clothes and papers.

Palmer, Mir, and González (2000) presented several methods for solving numerically the PDE governing Terzopoulos' deformable models and studied particularly its complexity and stability. These methods have been classified in explicit and semi-implicit methods using central finite difference methods and non-central finite difference methods. The author found that explicit methods are better than semi-implicit ones because of lower computational cost. Moreover, Palmer demonstrated that the behaviour of non-central finite difference methods is better because they are stable. The study was made for surfaces but can be easily extended to 3D curves and solids. The applications were illustrated by the animation of a held handkerchief and the free fall of a tablecloth.

Bruniaux, Ghith, and Vasseur (2003) used Terzopoulos' deformable models to simulate and study woven fabrics behaviour. A great importance was given to the identification of physical and mechanical parameters of textile fabrics necessary to adapt the model to woven fabrics. The results seem to be qualitatively convincing. However, the authors did not develop the numerical implementation of the model and did not give any indication about boundary conditions applied in their simulations.

In this paper, a general formulation of deformable models for woven fabrics modelling is presented, taking into account the specific characteristics of textile fabrics. The numerical resolution of the PDEs controlling the model are made using the FEM. Simulations of fabrics dynamic behaviour are also presented. A great interest is devoted to the drape behaviour of woven fabrics.

In the following paragraph, we present the general formulation of deformable models by indicating mathematical, geometrical and mechanical concepts, leading to a better understanding of the formulation. Numerical implementation of deformable models is introduced in the third paragraph. Some preliminary numerical results are also discussed. The last part is devoted to experimental results, which are presented and compared with some numerical ones.

Basic formulation

We denote by $\Phi = (O, \vec{i}, \vec{j}, \vec{k})$ the inertial frame. Time is indicated by the independent variable $t \geq 0$.

Parametric representation of fabric surface

Textile woven fabric is assumed as a surface S in which the thickness ($\delta > 0$) can be neglected by comparison with two other dimensions: length ($L > 0$) and width ($l > 0$). This surface is defined by its parametric representation:

$$\begin{aligned} &\vec{r^t}: \Omega \subset R^2 \to S \subset R^3 \\ &(a_1, a_2) \mapsto (x_1, x_2, x_3). \end{aligned} \tag{1}$$

So, $x_i = x_i(a_1, a_2)$, and $\vec{r^t} = [x_1\ x_2\ x_3]^T$ is the vector of instantaneous position of a point P belonging to surface S at time $t > 0$. The parametric field is defined by $\Omega = \{(a_1, a_2) \in R^2, |a_1| \leq L/2, |a_2| \leq l/2\}$. The fabric is characterised by the interlacing of two sets of perpendicular yarns: warp (L_{warp}) and weft (L_{weft}) directions parameterised, respectively, by a_1 and a_2.

$$\begin{aligned} L_{\text{warp}} &= \{(a_1, a_2) \in R^2, |a_1| \leq L/2, a_2 = C_1\} \\ L_{\text{weft}} &= \{(a_1, a_2) \in R^2, |a_2| \leq l/2, a_1 = C_2\}. \end{aligned} \tag{2}$$

C_1 and C_2 are two real constants. Figure 1 shows an illustration of surface fabric parameterisation.

Fabric deformations

A surface is subjected to two types of elastic deformations: stretching and bending. The elastic strain relating to stretch can be introduced by the first fundamental form of surface. The second fundamental form gives a measurement of the elastic strain due to bending. These two fundamental forms are given by the following formula (Manuel & Paulo, 1989):

$$\begin{aligned} \mathrm{I} = d\vec{r} \cdot d\vec{r} &= \sum_{\alpha,\beta=1}^{2} g_{\alpha\beta} \cdot da_\alpha da_\beta; \prod = -d\vec{r} \cdot d\vec{n} \\ &= \sum_{\alpha,\beta=1}^{2} b_{\alpha\beta} \cdot da_\alpha da_\beta. \end{aligned} \tag{3}$$

To describe these deformations, two tensors of surface are used: Euclidian tensor G and curvature tensor B.

$$\begin{aligned} G = \left(g_{\alpha\beta}\right)_{1\leq\alpha,\beta\leq 2}, g_{\alpha\beta} &= \frac{\partial \vec{r}}{\partial a_\alpha} \cdot \frac{\partial \vec{r}}{\partial a_\beta}; B = \left(b_{\alpha\beta}\right)_{1\leq\alpha,\beta\leq 2}, \\ b_{\alpha\beta} &= \frac{\partial^2 \vec{r}}{\partial a_a \partial a_\beta} \cdot \vec{n} \end{aligned} \tag{4}$$

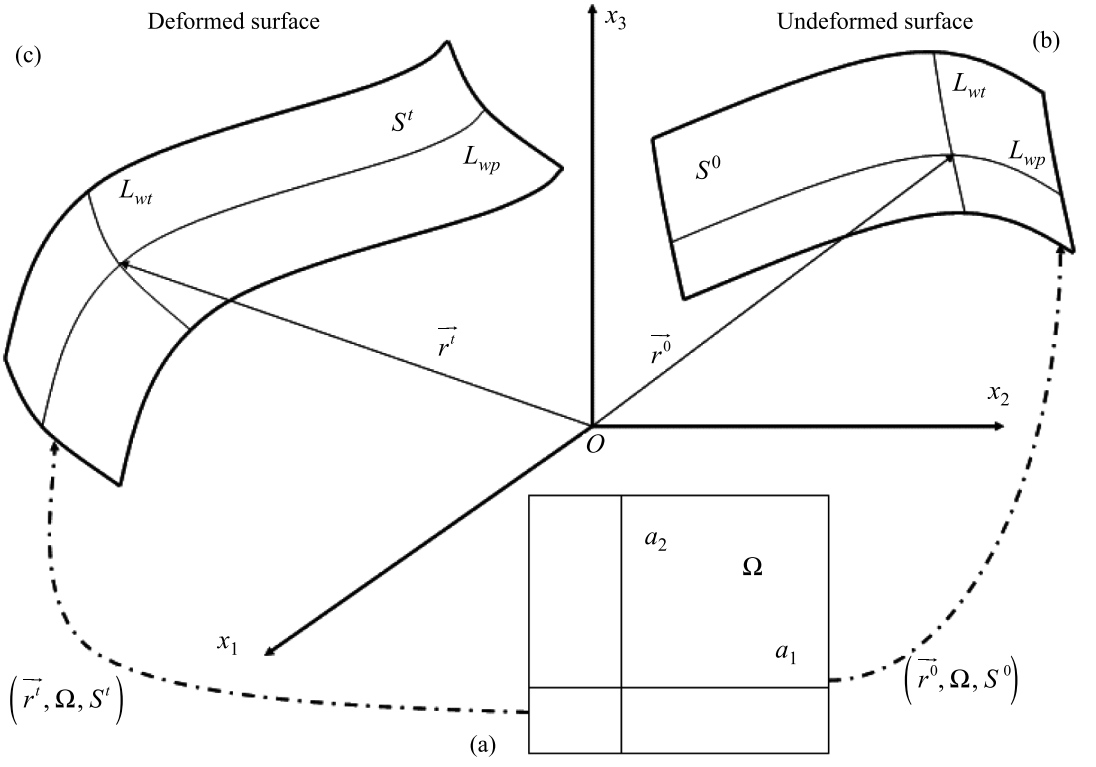

Figure 1. Surface parameterization: (a) parametric field, (b) initial configuration, and (c) current configuration.

where $\vec{n}$ is the unit normal of surface:

$$\vec{n} = \frac{\partial \vec{r}}{\partial a_1} \times \frac{\partial \vec{r}}{\partial a_2} \Big/ \left\| \frac{\partial \vec{r}}{\partial a_1} \times \frac{\partial \vec{r}}{\partial a_2} \right\|.$$

Initial configuration, at $t = t_0$, is given by the map $(\vec{r}^0, \Omega, S^0)$. We associate, for surface S^0, two metric tensors: G^0 and B^0. At current time $t > t_0$, surface configuration is given by the map $(\vec{r}^t, \Omega, S^t)$. Metric tensors associated to current surface S^t are given by G^t and B^t. Fabric deformations are illustrated in Figure 2.

Energy of deformation

Two types of elastic deformation energies are considered: energy due to the stretching or/and shearing deformations (ε^s) and energy related to bending deformations (ε^b). The first one is due to the variation of Euclidian metric tensor between initial and current configurations. It can be formulated as:

$$\varepsilon^s(\vec{r}) = \iint_\Omega \left\| G^t - G^0 \right\|_{w^s}^2 da_1 da_2 \tag{5}$$

where $\left\| G^t - G^0 \right\|_{w^s}^2$ indicates the Hilbert–Schmidt norm of the metric tensor variation weighted by the coefficients of the matrix W^s. It can be calculated as following:

$$\left\| G^t - G^0 \right\|_{w^s}^2 = \sum_{\alpha,\beta=1}^{2} w_{\alpha\beta}^s \cdot \left(g_{\alpha\beta}^t - g_{\alpha\beta}^0 \right)^2. \tag{6}$$

The second one is related to the variation of curvature tensor between initial and current configurations. It can be computed as:

$$\varepsilon^b(\vec{r}) = \iint_\Omega \left\| B^t - B^0 \right\|_{w^b}^2 da_1 da_2. \tag{7}$$

Same derivation can be used for curvature deformation energy, and we obtain:

$$\left\| B^t - B^0 \right\|_{w^b}^2 = \sum_{\alpha,\beta=1}^{2} w_{\alpha\beta}^b \cdot \left(b_{\alpha\beta}^t - b_{\alpha\beta}^0 \right)^2. \tag{8}$$

So, the internal deformation measurement is given by:

$$\varepsilon(\vec{r}) = \iint_\Omega \left(\sum_{\alpha=1}^{2} \sum_{\beta=1}^{2} w_{\alpha\beta}^s \cdot \left(g_{\alpha\beta}^t - g_{\alpha\beta}^0 \right)^2 + w_{\alpha\beta}^b \cdot \left(b_{\alpha\beta}^t - b_{\alpha\beta}^0 \right)^2 \right) da_1 da_2. \tag{9}$$

Taking first the variation of the energy functional (Ciarlet, 2005; Goldstein, Poole, & Safko, 2000; Kravchuk & Neittaanmäki, 2007), we obtain the expression of internal forces:

$$\frac{\delta \varepsilon(\vec{r})}{\delta \tilde{r}} = -\sum_{\alpha=1}^{2} \sum_{\beta=1}^{2} \frac{\partial}{\partial a_\alpha} \left(S_{\alpha\beta} \cdot \frac{\partial \vec{r}}{\partial a_\beta} \right) + \sum_{\alpha=1}^{2} \sum_{\beta=1}^{2} \frac{\partial^2}{\partial a_\alpha \partial a_\beta} \left(C_{\alpha\beta} \cdot \frac{\partial^2 \vec{r}}{\partial a_\alpha \partial a_\beta} \right). \tag{10}$$

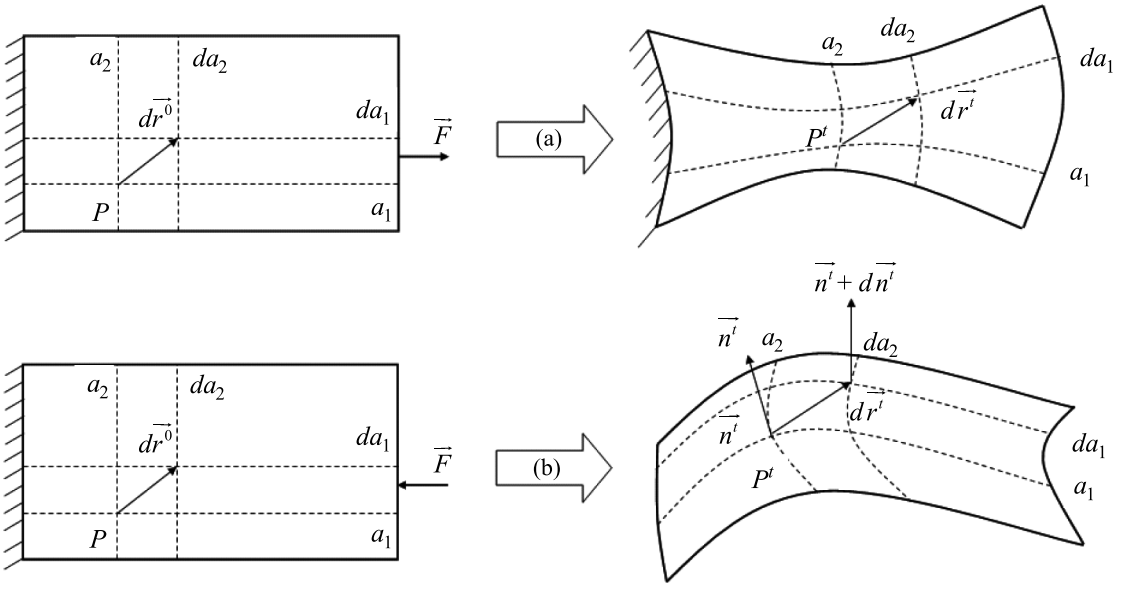

Figure 2. Surface deformations: (a) stretching–shearing and (b) bending.

In this expression, we have

$$S_{\alpha\beta} = w^s_{\alpha\beta}\left(g^t_{\alpha\beta} - g^0_{\alpha\beta}\right) \text{ and } C_{\alpha\beta} = w^b_{\alpha\beta}\left(b^t_{\alpha\beta} - b^0_{\alpha\beta}\right).$$

These coefficients describe the following material properties: $w^s{}_{\alpha\beta}$ for stretch– shear behaviour, and $w^b{}_{\alpha\beta}$ for bending.

General deformable model formulation

The equations governing the motion and the dynamic behaviour of fabrics are obtained in virtue of the First Dynamic Principle.

$$\frac{\partial}{\partial t}\left(\rho\frac{\partial\vec{r}}{\partial t}\right) + \mu\frac{\partial\vec{r}}{\partial t} + \frac{\delta\varepsilon\left(\vec{r}\right)}{\delta\vec{r}} = \overrightarrow{F^{\text{ext}}} \tag{11}$$

where ρ is the surface mass density (kg m^{-2}) and μ is the damping density (kg m^{-2} s^{-1}). In Equation (11), we distinguish the following terms:

- Inertial forces: $\overrightarrow{F^{\text{ine}}} = \frac{\partial}{\partial t}\left(\rho\frac{\partial\vec{r}}{\partial t}\right)$
- Forces due to viscous damping: $\overrightarrow{F^{\text{dam}}} = \mu\frac{\partial\vec{r}}{\partial t}$

In this study, the viscous damping force is treated by adding the resistant-force vector into the external-load vector. It is taken equal to 10% of the instantaneous velocity of fabric. So,

$$\left\|\overrightarrow{F^{\text{dam}}}\right\| = \mu\cdot\left\|\frac{\partial\vec{r}}{\partial t}\right\| \text{ and } \mu = -0.1\ \text{kg m}^{-2}\text{s}^{-1}$$

- Forces due to internal elastic energies:

$$\overrightarrow{F^{\text{int}}} = \frac{\delta\varepsilon\left(\vec{r}\right)}{\delta\vec{r}}$$

- External forces: $\overrightarrow{F^{\text{ext}}}$ due to gravity $\overrightarrow{F^{\text{g}}} = \rho.\vec{g}$ ($\vec{g}$ is the gravity acceleration) and due to air flow

$$\overrightarrow{F^{\text{air}}} = C\left[\vec{n}.\left(\vec{u} - \frac{\partial\vec{r}}{\partial t}\right)\right]\vec{n}$$

(C is the fluid damping and $\vec{u}$ is the average fluid velocity)

Model coefficients identification

We consider that the fabric has an orthotropic elastic behaviour. To describe the stretch–shearing behaviour of the textile material, we use its rigidity in the two directions of orthotropy (warp and weft directions), and these two Poisson ratios. In this approach, we will take:

$$w^s_{11} = E_{wp}, w^s_{12} = H, w^s_{21} = H, w^s_{22} = E_{wt} \tag{12}$$

where E_{wp} and E_{wt} are Young's modulus in warp and weft direction, respectively. The modulus of rigidity is denoted by H. In the same way, we define coefficients related to bending behaviour as:

$$w^b_{11} = Rf_{wp}, w^b_{12} = w^b_{21} = 0, w^b_{22} = Rf_{wt} \tag{13}$$

where Rf_{wp} and Rf_{wt} are the flexural rigidity in warp and weft direction, respectively. The coefficients w^b_{12} and w^b_{21} represent the twisting strength. In this work, this kind of deformation is neglected. So, these coefficients are taken equal to zero. All simulations are made with boundary conditions that do not allow twisting deformations.

Numerical implementation

In this section, the numerical implementation of deformable models is developed. The FEM is used to solve the PDEs governing the behaviour of textile materials.

Problem definition

The PDEs describing the textile materials behaviour are given by Equation (11). In this formulation, inertial, damping and internal forces are balanced by external forces acting on the fabric surface. These forces cause deformations and motion of fabric surface with time. The fabric surface is subdivided into curvilinear triangular finite elements. By solving Equation (11), we obtain for every time step the vector of instantaneous position of all mesh points. Time discretisation is made by subdividing the whole time interval into infinitesimal time steps.

Algorithm of FEM resolution

The PDEs, which must be solved, present two aspects: they are evolutionary and non-linear. The algorithm allows an incremental solution of these equations and makes them linear. The linearisation is done by updating fabric configuration in each time step, namely metric tensors and normal vectors. The incrementing of time is done only after ensuring the minimisation of internal energy of deformation. This is carried out in an iterative way. The used algorithm is illustrated in Figure 3.

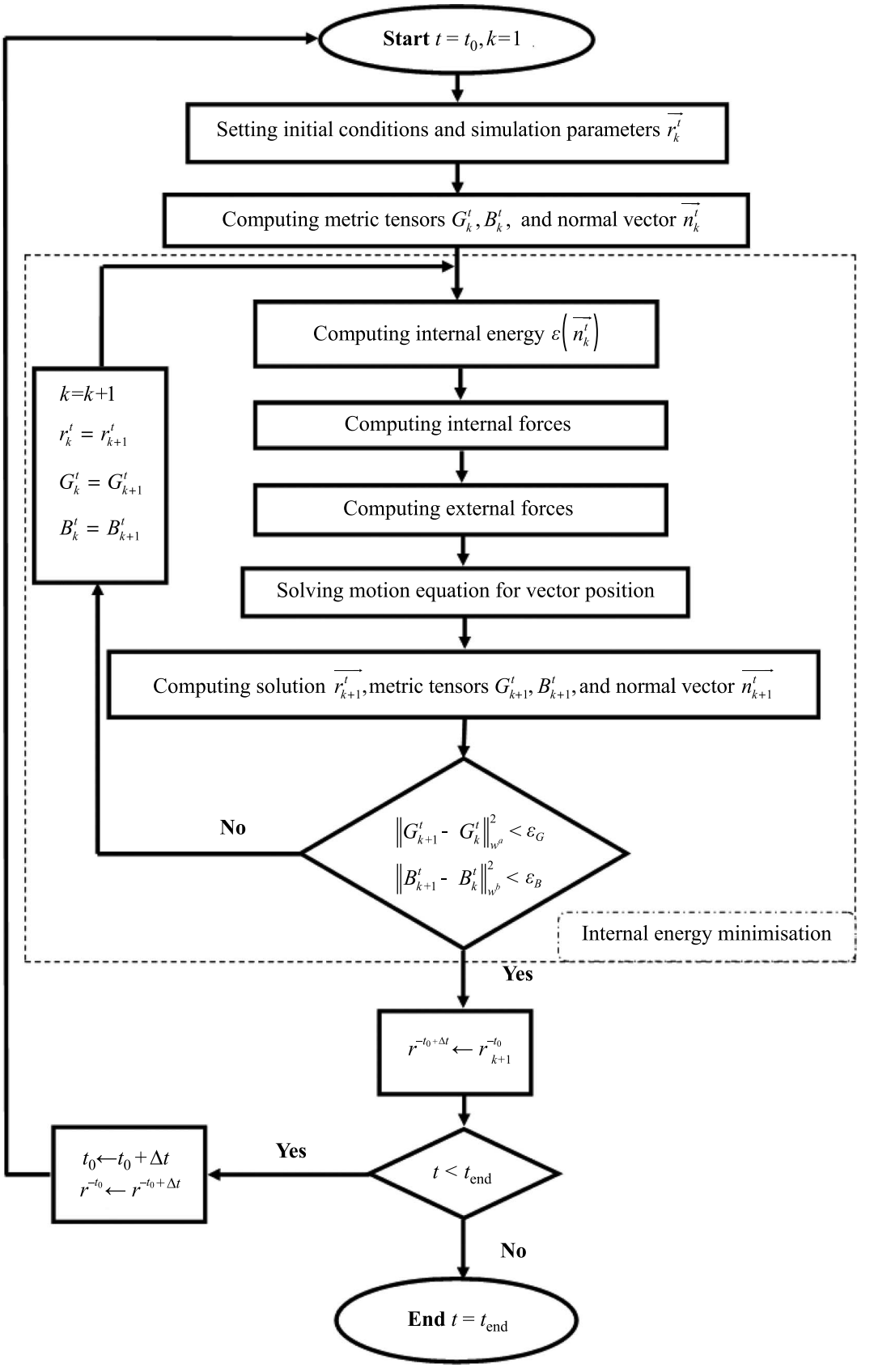

Figure 3. The FEM resolution algorithm.

The code is composed of two loops: a principal loop, which integrates the equations of the model according to time, and a sub-loop, which minimizes the internal energy of deformation of fabric. The principal loop is explicit. Assuming that mass density does not depend on time, Equation (11) can be written as:

$$\rho\frac{\partial^2\vec{r}}{\partial t^2}+\mu\frac{\partial\vec{r}}{\partial t}+\overrightarrow{F^{\text{int}}}=\overrightarrow{F^{\text{ext}}}. \tag{14}$$

For each node point, the time derivatives of instantaneous position vector are approximated by the discrete central difference as follows:

$$\frac{\partial^2\vec{r}}{\partial t^2}=\frac{\vec{r}^{\,t+\Delta t}-2\vec{r}^{\,t}+\vec{r}^{\,t-\Delta t}}{\Delta t^2}$$
$$\frac{\partial\vec{r}}{\partial t}=\frac{\vec{r}^{\,t+\Delta t}-\vec{r}^{\,t-\Delta t}}{2\Delta t},\ \vec{v}=\frac{\vec{r}^{\,t}-\vec{r}^{\,t-\Delta t}}{\Delta t}. \tag{15}$$

Substituting Equation (15) into Equation (14) leads to the explicit scheme as follows:

$$\vec{r}^{\,t+\Delta t}=\left(\frac{\rho}{\Delta t^2}+\frac{\mu}{2\Delta t}\right)^{-1}\left(\overrightarrow{F^{\text{ext}}}^{t}-\overrightarrow{F^{\text{int}}}^{t}\right.$$
$$\left.+\left(\frac{\rho}{\Delta t^2}+\frac{\mu}{2\Delta t}\right)\vec{r}^{\,t}+\left(\frac{\rho}{\Delta t}-\frac{\mu}{2}\right)\vec{v}^{\,t}\right). \tag{16}$$

Equation (16) is used for computing new positions, at time $t + \Delta t$, of all mesh nodes using an explicit step-by-step integration method. In this equation, $\vec{\vec{v}}^{\,t}$ is the vector of instantaneous velocity.

To decide the minimisation of internal energy at each time increment, we carry out a test relating to the variation of the metric tensors G and B between two iterations k and $k + 1$. If these variations are lower than ε_G and ε_B, respectively i.e.,

$$\left\|G_{k+1}^t-G_k^t\right\|<\varepsilon_G \text{ and } \left\|B_{k+1}^t-B_k^t\right\|<\varepsilon_B,$$

then energy is minimal for this increment of time. If not, we reiterate until this condition is reached. For all reported simulations, $\varepsilon_G = \varepsilon_B = 10^{-3}$.

Some preliminary numerical results

Contact treatment

When the fabric is in contact with a rigid object such as a table, a mannequin or the human body, it is necessary to take into account this type of interaction. We note also that some parts of the fabric can come in contact with other parts of the same fabric. In this work, we tested two methods to solve the problem of contact in fabric simulations draped on tables of various geometries.

The first method is to disregard the part which is in contact with the table and consider only that part which is not in contact with the rigid object. In the second method, we deal with the problem of contact by using an algorithm which controls the points in contact with the table. The used algorithm is illustrated in Figure 4.

The results obtained from these two methods are illustrated in Figure 5. We note that the differences between these results are not significant. However, we estimate that for contacts with more complex geometry, the first method ceases to be correct. In the remainder of simulations, the second method for contact treatment is used.

Some numerical simulations

In this part, we consider a fabric of dimensions 200 mm × 200 mm draped over a square table of dimensions

Algorithm of contact

Required : Table dimension in x_1 direction : Dx_1
Table dimension in x_2 direction : Dx_2
Domain of contact: D
Point : $P(x_1, x_2, x_3)$

for $P \in D$ do

if $\left\{\begin{array}{c}\left|x_1^{t+\Delta t}(P)\right|<D_{x_1}\text{and}\left|x_2^{t+\Delta t}(P)\right|<D_{x_1}\\ \text{and } x_1^{t+\Delta t}(P)<x_2^0(P)\end{array}\right\}$ then

$x_3^{t+\Delta t}(P)=x_3^0(P)$

end

end;

(a)

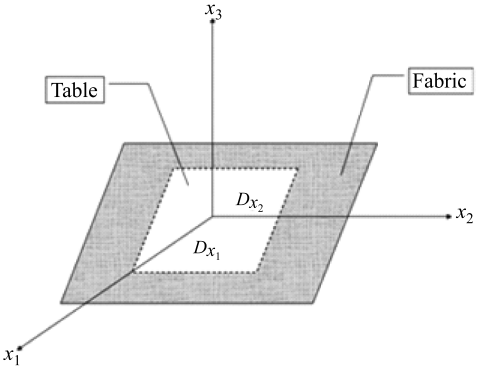

(b)

Figure 4. Contact treatment: (a) pseudo-algorithm of contact and (b) contact illustration.

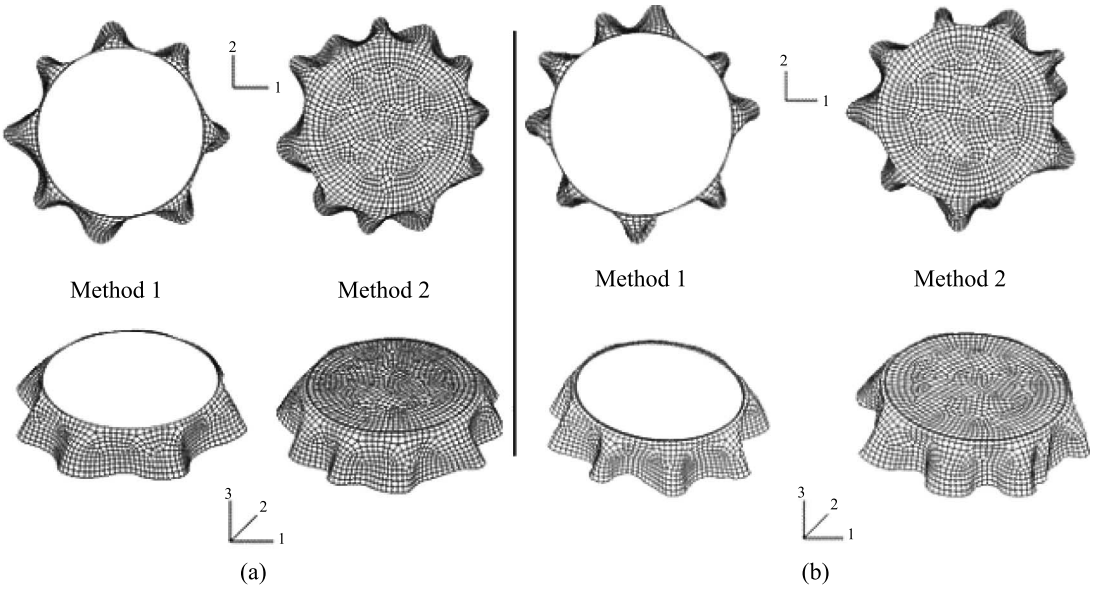

Figure 5. Comparison between two methods for contact treatment: (a) plain and (b) twill fabric.

100 mm × 100 mm. The fabric is subjected only to the action of its own weight. In Figure 6, three fabrics (F1, F5 and F9) are simulated. In these simulations, we notice the effect of the weave pattern on the drapeability of fabrics. Indeed, the aspect obtained on satin fabric (F9) is more convincing visually. The formation of the nodes at the corners of the table is much fuller for this fabric. This can be explained by the low bending stiffness of fabric F9 compared with fabric F1 (plain weave), and less slightly with fabric F5 (twill weave).

Figure 7 shows the displacements of the corner point A obtained in these simulations. We state that the

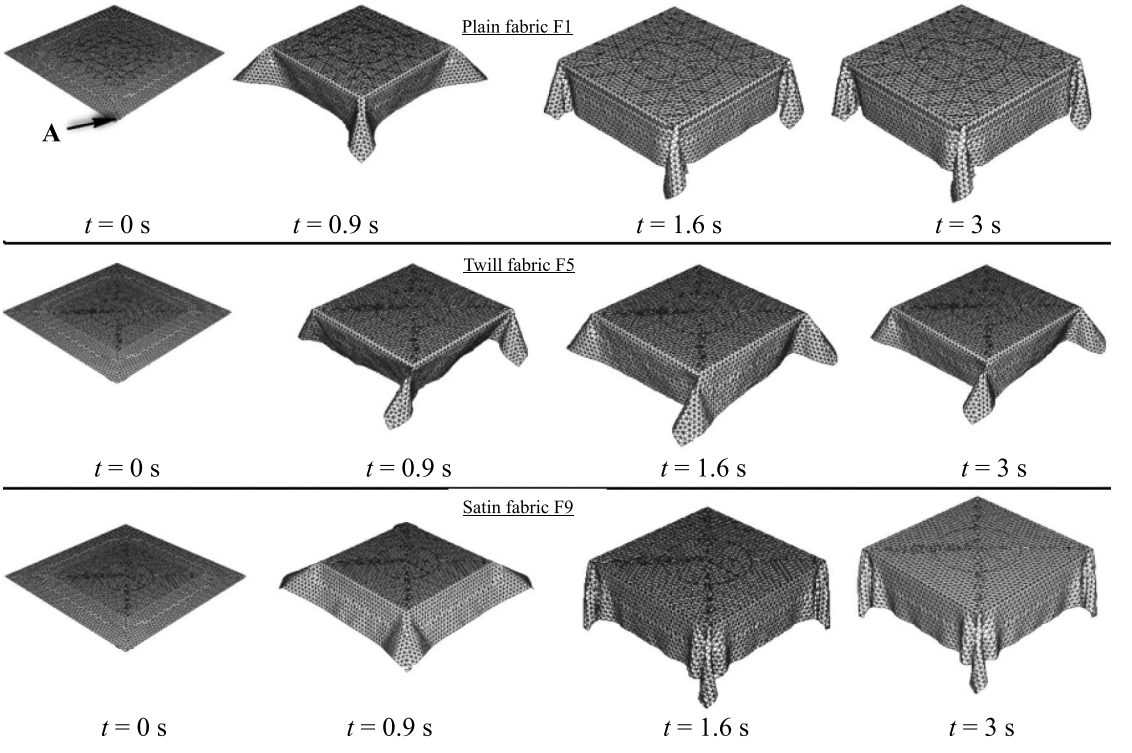

Figure 6. Fabric draped over rectangular table: plain (F1), twill (F5) and satin (F9) fabric.

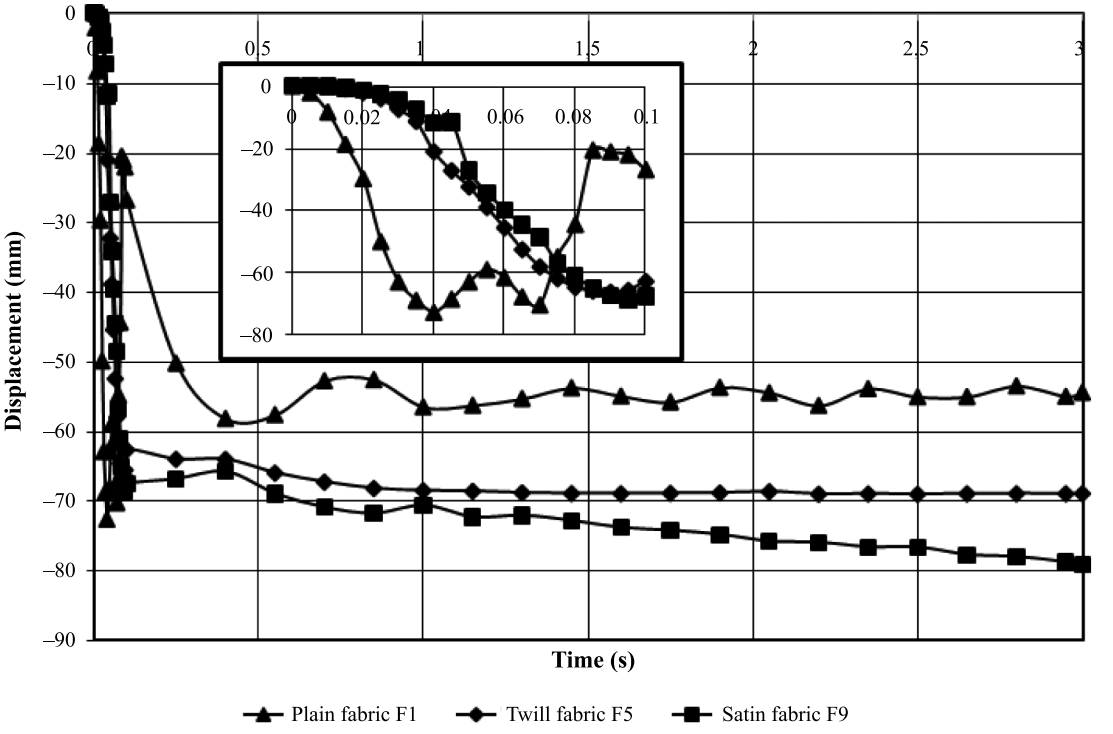

Figure 7. Displacement of the corner point A of three fabrics: plain (F1), twill (F5) and satin (F9) fabric.

fabrics reach the maximum displacement very quickly (in at least of 0.1 s). We note that during this time, the behaviour of the fabrics is unstable (e.g. there are fluctuations which are significant especially for fabric F1; see zoomed figure). The stabilisation of the configuration is obtained for the fabrics F5 and F9 after 0.5 s. As for fabric F1, the configuration starts to become stabilised after 1 s. This can be explained by the rigidity of plain fabric F1, which makes it difficult to deform this fabric and hence the fabric takes the shape of the table. All these simulations are made using 5750 curvilinear triangular elements, except for simulation presented in Figure 9, in which 4226 quadrilateral finite elements are used.

In Figure 8, we simulate fabric F1 under the same conditions as previously but this time the fabric is subjected to an air flow for a certain duration of time then the air flow is stopped. Then, the fabric is again subjected to the air flow by changing its direction. For the first configuration, the direction of the air flow is

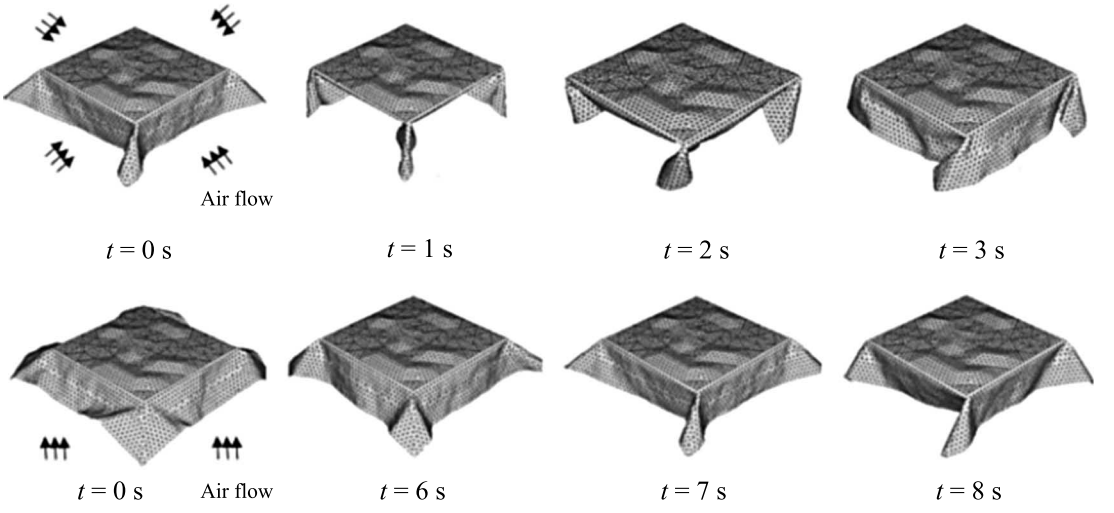

Figure 8. Plain fabric (F1) draped over rectangular table and subjected to moderate air flow.

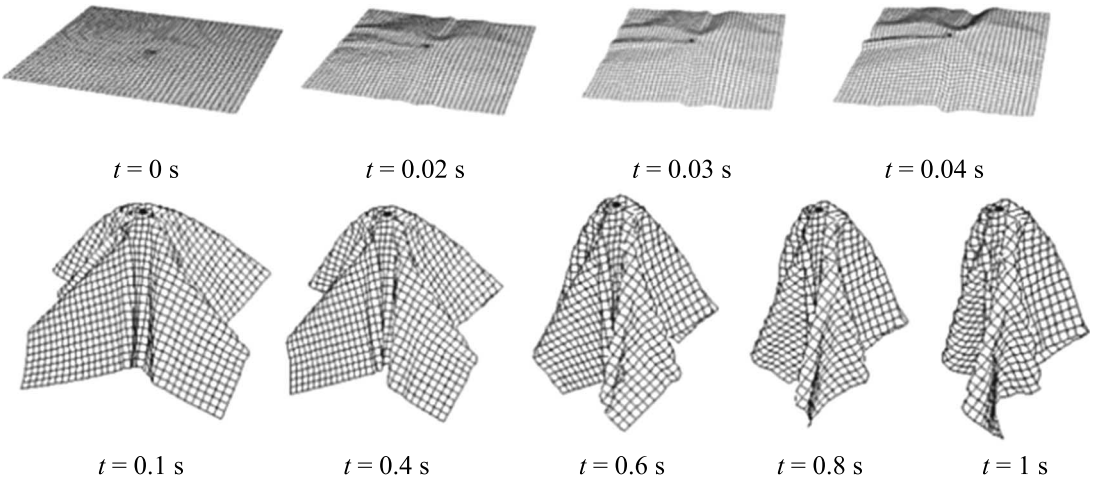

Figure 9. Plain fabric (F1) constrained at one of its points.

opposed to the initial normal of each falling part of fabric:

$$\vec{u} = -\left\|\frac{\partial \vec{r}}{\partial t}\right\| \cdot \vec{n} \text{ and } C = 0.03 \text{ kg m}^{-2}.$$

For the second configuration,

$$\vec{u} = -\left\|\frac{\partial \vec{r}}{\partial t}\right\| \cdot \vec{k} \text{ and } C = 0.03 \text{ kg m}^{-2}.$$

This example shows the capacity of our model to reproduce the fabric response to the action of air flow. The model reproduces the strong change in the air flow direction with efficiency.

In Figure 9, we present a simulation of fall for fabric F1 which is constrained at one of these points.

When there are self-collisions, the mesh is destroyed and calculations do not converge. To avoid this problem, a re-meshing of the structure is carried out. The simulations presented in this work are obtained after optimising the meshing and the time steps to eliminate problems due to self-collisions. We estimate that the minimisation of internal energy would contribute to avoiding these self-collisions, which are characterised by the local increase in the deformation energy. We are working to incorporate into our FEM algorithm a subroutine which handles these self-collisions.

Experimental study

Experimental fabric characterisation

The experimental study is carried out with 12 fabrics of different structures and compositions. For each one, some mechanical and physical characteristics are identified by using several tests.

Parameters related to the composition and construction

In this section, some parameters related to fabric structure such as fabric pattern, composition, yarn density and yarn count are identified. These parameters are summarised in Table 1.

Physical and mechanical parameters

Physical parameters of fabrics such as mass density and thickness are identified. To determine Young's modulus in warp, weft and bias directions, tensile tests are carried out until rupture. A fabric specimen of dimensions 200 mm × 50 mm (Figure 10) is subjected to traction until rupture by means of a suitable testing device (universal tensile testing machine). Tests are carried out on five specimens for each direction (warp, weft and bias directions).

The Poisson ratio represents the quotient between transversal contraction and longitudinal dilation. A method to determine the Poisson ratio for textile fabrics is to use a tensile threshold test (Bruniaux et al., 2003). The principle of this test is as follows: as for the preceding test, a fabric specimen of dimensions 200 mm × 50 mm is used on which a rectangle of known dimensions (a, b) is drawn (Figure 10(d)), then the fabric specimen is subjected to tensile test until elongation (with a fixed value: 3% of breaking strain). So, the dimensions of the rectangle become equal to $a + \delta a$ and $b - \delta b$. Measurements must be taken directly subsequent to the test to avoid fabric relaxation. The Poisson ratio can be estimated by:

$$\nu = \frac{\delta b}{\delta a}. \quad (17)$$

The modulus of rigidity H is computed using the following formula (Saville, 1999, p. 272).

Table 1. Parameters related to the fabric composition and construction.

	Pattern fabric		Yarn count		Yarn density		Composition	
Fabric code	Name	Scheme	Warp (end/cm)	Weft (picks/cm)	Warp (tex)	Weft (tex)	Warp	Weft
F1			16	32	20	26	Cotton	Cotton
F2	Plain		22	21	30	28	Cotton	Polyester
F3			20	18	40	28	Polyester	Cotton
F4			24	18	43	31	Polyester	Polyester
F5			20	22	30	30	Cotton	Cotton
F6	Twill		25	27	31	30	Cotton	Polyester
F7			22	30	33	36	Polyester	Cotton
F8			20	28	30	34	Polyester	Polyester
F9			22	31	28	28	Cotton	Cotton
F10	Satin		24	26	24	30	Cotton	Polyester
F11			34	32	22	28	Polyester	Cotton
F12			36	34	26	30	Polyester	Polyester

$$\frac{1}{H} = \frac{4}{E_{45}} - \frac{1-\nu_2}{E_1} - \frac{1-\nu_1}{E_2} \tag{18}$$

where E_1, E_2 and E_{45} are Young's moduli in the warp, weft and bias directions, respectively, and ν_1 and ν_2 are the fabric Poisson ratios. The results of these tests are mentioned in Table 2.

The bending behaviour of fabrics is described by using two flexural rigidity moduli in warp and weft directions. The cantilever stiffness test is used to determine the bending length in warp and weft directions. In this test, a horizontal fabric specimen of dimensions 200 mm × 25 mm is clamped at one end and the rest of the strip is allowed to hang under its own weight until it reaches a plane inclined at an angle θ = 41.5°. The principle of this test is illustrated in Figure 11. The test is carried out on five specimens for each direction (warp and weft directions). The bending length is related to the angle that the fabric makes to the horizontal by the following relation (Saville, 1999, p. 257):

$$C = L\left(\frac{\cos(0.5\times\theta)}{8\tan\theta}\right)^{\frac{1}{3}} \tag{19}$$

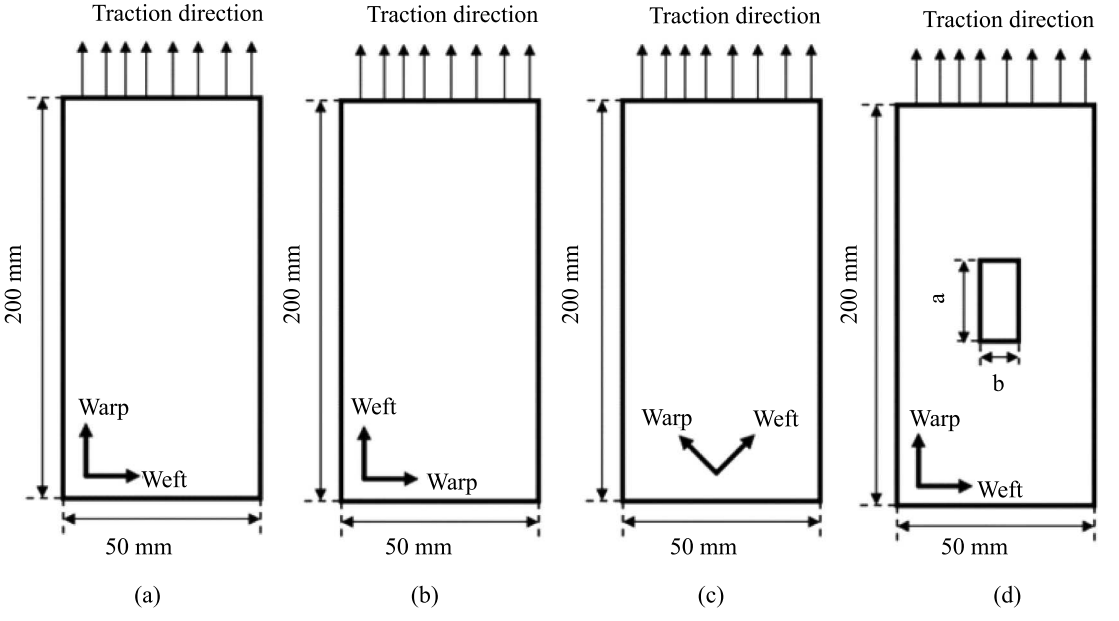

Figure 10. Mechanical properties characterisation: (a) warp, (b) weft, (c) bias direction and (d) Poisson ratio.

Table 2. Physical and mechanical fabric properties.

Fabric code	Warp direction			Weft direction						
	Young's modulus	Poisson ratio	Flexural rigidity modulus	Young's modulus	Poisson ratio	Flexural rigidity modulus	Bias Young's modulus	Shear rigidity	Mass density	Thickness
	E_{wp}	ν_{wp}	Rf_{wp}	E_{wt}	ν_{wt}	Rf_{wt}	E_{bias}	H	ρ	δ
	(MPa)		(μNm)	(MPa)		(μNm)	(MPa)	(MPa)	(g·m^{-2})	(mm)
F1	6.33	0.3	25.21	2.55	0.4	33.46	4.36	1.82	198	0.49
F2	7.30	0.3	21.59	2.39	0.4	20.40	4.56	1.99	203	0.46
F3	6.41	0.3	21.36	3.17	0.4	17.99	4.73	1.89	200	0.48
F4	7.56	0.3	12.56	4.15	0.3	16.45	5.34	2.05	179	0.43
F5	2.47	0.3	11.38	1.67	0.4	11.06	2.70	1.22	187	0.47
F6	4.34	0.3	6.80	1.14	0.3	10	2.87	1.62	189	0.57
F7	1.79	0.4	7.26	2.26	0.3	5.93	2.68	1.20	191	0.62
F8	3.36	0.3	8.28	2.03	0.4	8.66	3.17	1.35	188	0.58
F9	2.00	0.4	5.93	1.29	0.4	6.98	2.45	1.15	188	0.62
F10	5.59	0.3	10.53	1.45	0.4	6.62	3.51	1.82	184	0.57
F11	2.21	0.3	6.07	2.29	0.3	8.16	2.81	1.25	186	0.68
F12	4.76	0.3	9.74	2.03	0.3	9.05	3.44	1.49	187	0.58

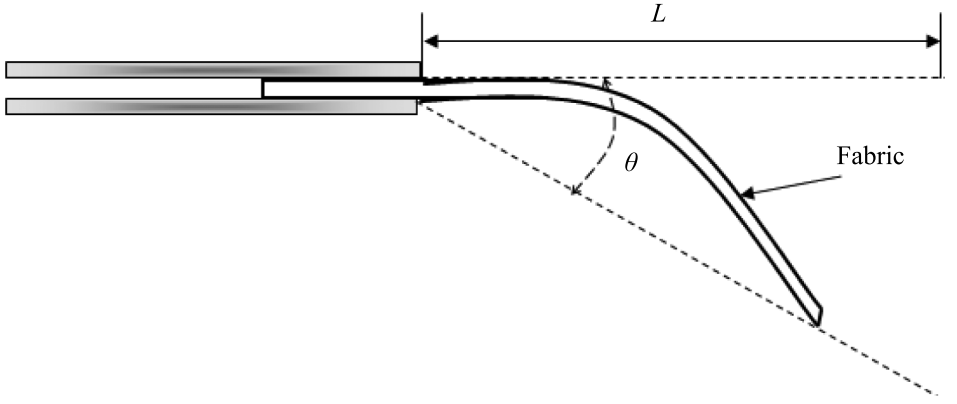

Figure 11. Principle of cantilever stiffness test.

where L is the length of the fabric projecting, θ is the angle the fabric bends to, and ρ (g m^{-2}) is the mass density of the fabric. The bending length in warp direction (respectively weft direction) is correlated to flexural rigidity modulus in warp direction (respectively weft direction) by the following formula (Saville, 1999, p. 259):

$$Rf_{wp} = 9.807 \times \rho \times C_{wp}^3 \times 10^{-6}$$
$$Rf_{wt} = 9.807 \times \rho \times C_{wt}^3 \times 10^{-6} \quad (20)$$

where Rf_{wp} (μNm) and Rf_{wt} (μNm) are the flexural rigidity moduli in warp and weft directions, C_{wp} (mm) and C_{wt} (mm) are the bending lengths in warp and weft directions.

Fabric drape evaluation

To determine fabric drape coefficients, traditional drape-meter is used (Figure 12(a)). The principle of this apparatus is: a circular fabric specimen of diameter 250 mm is placed on a support disc of diameter 150 mm, then a second disc of diameter 150 mm is placed at the concentric top of the specimen.

Measurements are taken after 15 minutes. We measure 16 rays on the specimen, as shown in Figure 12(b). Drape coefficient DC is calculated using the following formula:

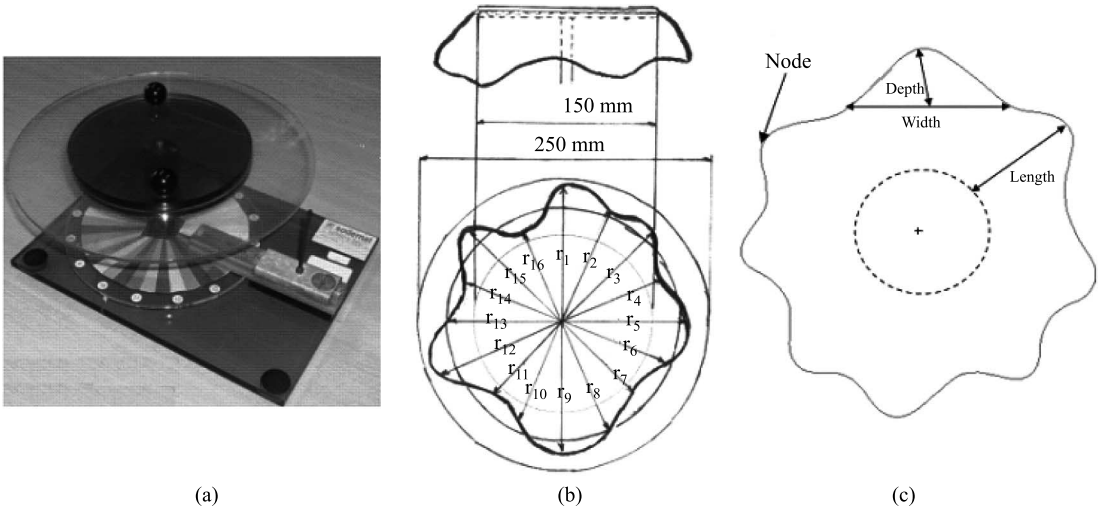

Figure 12. Characterisation of fabric drape: (a) drape-meter, (b) drape measurement and (c) node dimensions.

$$DC = \frac{S_c - S_i}{S_t - S_i} = \frac{d_m^2 - d_i^2}{d_t^2 - d_i^2} \quad (21)$$

where S_c represents the area of the circle of diameter d_m (in mm), d_m is the average of the 16 measured rays; S_i is the support disc area of diameter d_i = 150 mm, and S_t is the undeformed specimen area of diameter d_t = 250 mm.

We also characterised dimensions of the formed nodes. These dimensions are length, width and depth of the nodes. An illustration of these measurements is given in Figure 12(c). The results of these tests are mentioned in Table 3.

Results and discussion

Experimental vs. numerical results

In this section, the drape-meter test is simulated. For this purpose, a circular fabric of diameter 250 mm draped over a circular support disc of diameter 150 mm is simulated. The fabric is subjected only to the action of its weight. For the final fabric configuration, 16 rays

Table 3. Experimental fabric drape characterisation.

		Dimensions of nodes (mm)									
		Length			Width			Depth			
Fabric code	Node	Range	Mean	CV (%)	Range	Mean	CV (%)	Range	Mean	CV (%)	Drape coefficient *DC* (%)
F1	6	33–50	41.67	18.26	75–133	101.33	18.89	21–41	31.33	29.16	67
F2	5	37–46	43.40	9.16	95–147	114.80	17.71	26–43	35.20	21.77	67
F3	5	41–50	44.80	8.56	102–133	109	7.14	31–49	39.2	16.86	60
F4	6	38–46	42	6.02	67–133	102.83	21.95	17–38	27.83	27.68	63
F5	5	42–54	47.60	9.58	92–125	107.60	12.89	25–46	37.80	20.86	58
F6	5	32–63	43.60	26.43	89–125	105.20	15.30	18–45	34	30.35	64
F7	6	31–45	37.50	12.93	102–139	116.50	11.12	9–19	16.50	27.10	93
F8	6	42–50	48	6.97	70–141	101.50	25.91	8–31	19	42.89	92
F9	6	31–46	36	21.52	61–98	78.33	17.74	19–45	31.50	33.25	44
F10	6	29–46	36.29	16.51	50–83	69	16.63	25–42	32.71	17.71	25
F11	6	34–46	39.33	13.89	65–93	79	13.49	32–46	38	14.60	37
F12	6	38–46	40.67	8.03	40–129	91.33	39.18	8–44	28.67	51.77	59

Table 4. Numerical fabric drape characterisation.

Fabric code	Node	Dimensions of nodes (mm)									Drape coefficient *DC* (%)
		Length			Width			Depth			
		Range	Mean	CV (%)	Range	Mean	CV (%)	Range	Mean	CV (%)	
F1	7	42–50	46.57	5.93	63–102	88.43	15.94	20–39	28.43	25.19	68
F2	7	38–46	41.43	6.66	63–98	86.71	13.03	20–35	27.71	18.48	69
F3	7	38–58	45.43	17.19	47–105	84.29	24.07	23–47	33.29	31.69	63
F4	6	42–50	46.67	6.45	78–113	92.33	14.89	27–59	40.33	26.36	65
F5	7	46–70	55.71	14.27	56–109	88.29	22.26	24–52	35.43	28.73	60
F6	7	50–77	62	15.72	63–125	86	37.70	22–63	42.14	40.97	69
F7	7	28–54	43	23.45	63–147	97.57	34.27	9–36	19.14	55.24	94
F8	9	34–42	38.44	8.13	23–86	67.33	33.92	8–23	16.22	33.87	93
F9	8	39–61	45.13	15.64	45–83	60.63	18.87	23–49	37	25.11	46
F10	6	50–58	54.57	5.51	79–117	95.17	15.38	33–50	45.17	14.98	28
F11	7	46–54	51.14	7.44	60–97	74.57	16.01	36–52	43.43	12.39	35
F12	7	30–46	39.71	14.07	56–97	79.14	19.20	24–40	32.57	21.77	60

are measured from which the drape coefficient is calculated. The number and the dimensions of nodes are also determined. Results are reported in Table 4. These results are compared with those obtained in experiments. All these simulations are made using 5702 curvilinear triangular elements.

In Figure 13, we present the simulated configuration, the experimental configuration (photographed),

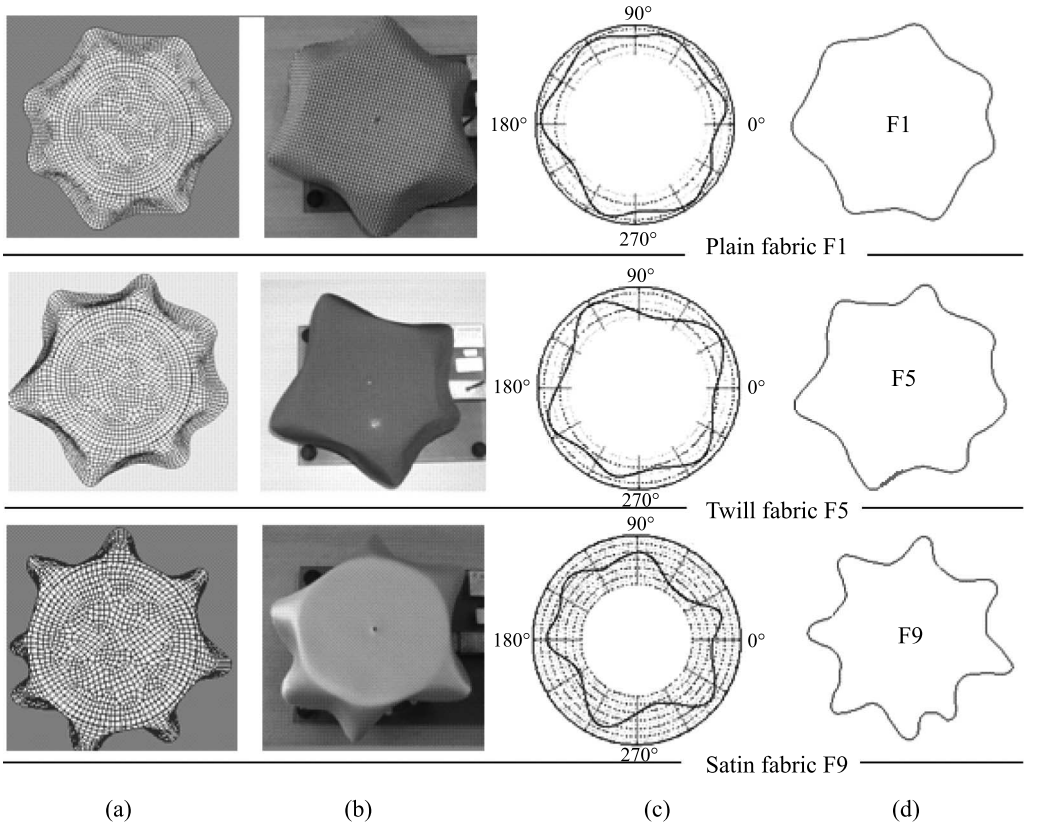

Figure 13. Comparison between experimental and numerical drape-meter test: (a) and (d), simulated; and (b) and (c), experimental results.

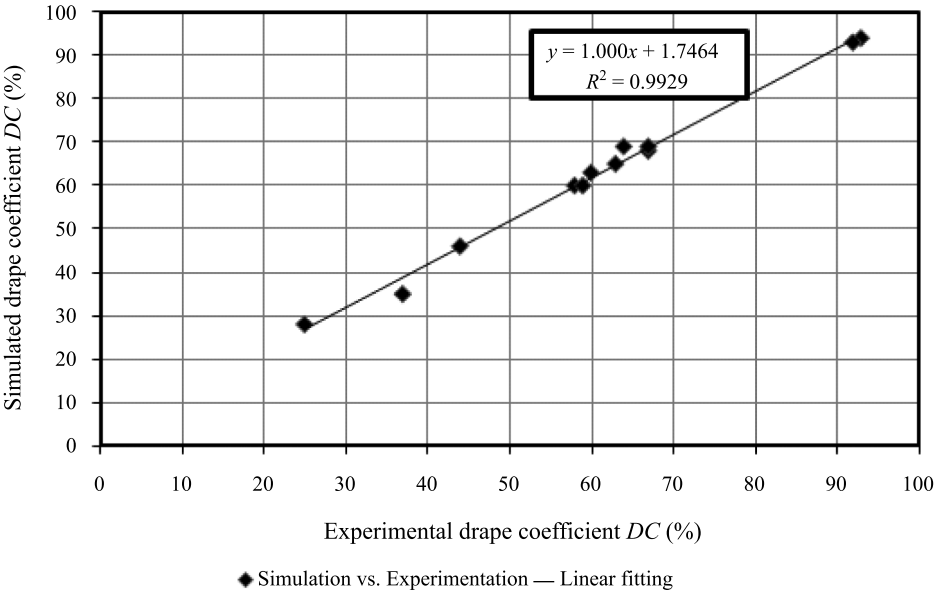

Figure 14. Correlation between experimental and numerical drape coefficient.

and the contours of the real and the simulated cases for the three fabrics.

Figure 14 shows the curve of correlation between the measured and the simulated drape coefficient. We obtain a significant coefficient of correlation (R = 0.9964). However, we note a difference between the real cases and the simulations concerning the number and the dimensions of nodes.

A comparison between the results obtained from real drape-meter and those obtained using virtual drape-meter is carried out. The comparison relates to the number of nodes (Figure 15) and their dimensions (Figure 16). For certain fabrics, we note that there is a small difference between the numbers of nodes actually obtained and those resulting from simulation. This can be explained by two reasons. The first lies in the fact that the self-collisions are not considered. Indeed, the distribution and the number of nodes are strongly influenced by the contact between the nodes. The second reason lies in the fact that the contact between the fabric and the support disc is considered without friction or slip, which is not always the case in reality.

Influence of some fabric parameters

Influence of coefficients related to stretch–shear and bending behaviour

In this section, we deal with the response of our model implementation when the coefficients of stretch behaviour and bending behaviour are modified. For this

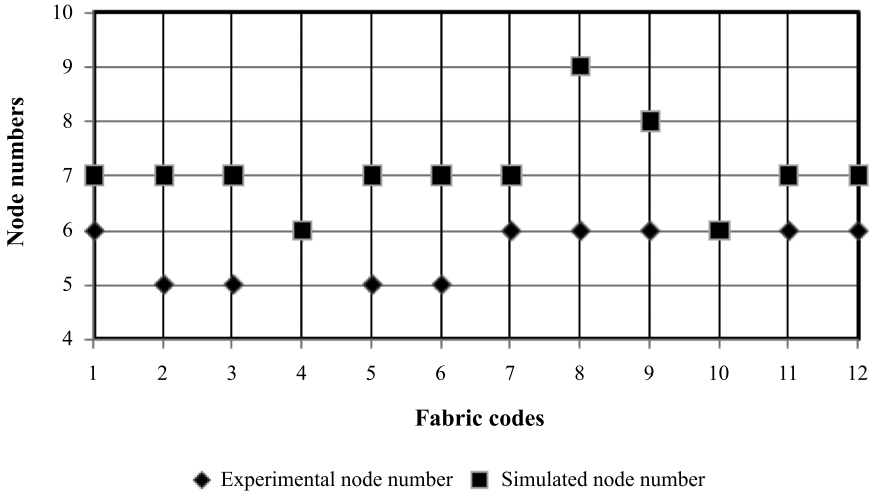

Figure 15. Comparison between experimental and numerical drape-meter test for node numbers.

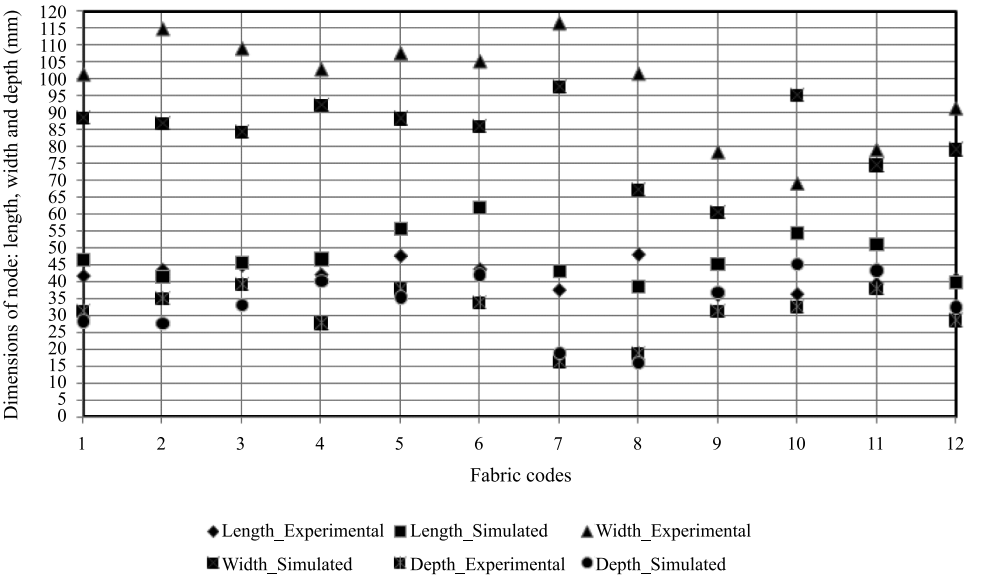

Figure 16. Comparison between experimental and numerical drape-meter test for some drape attributes (length, width and depth).

purpose, we have simulated different fabrics with various mechanical properties. In Figure 17, we present the response of three different fabrics having different coefficients related to the stretch–shear behaviour. Fabrics F4-A and F4-B have the same characteristics as those of fabric F4 except for the parameters related to the stretch–shear behaviour, which are taken equal to those of F12 and F7, respectively. In all these simulations, a square fabric of dimensions 200 mm × 200 mm is constrained at three edges. The fourth edge is free. In Figure 18, we present the x_3-displacement of the middle point (point A). The fabric is subjected to the action of its weight. Simulations are made for a duration of 1 s, with a fixed time step of 0.001 s.

The same simulations are made for the three fabrics having different bending coefficients. Fabrics F1-A and F1-B have the same characteristics as those of fabric F1 except for the parameters related to the bending behaviour, which are taken equal to those of F5 and F11, respectively. In Figures 19 and 20, we present the results of these investigations. In all these simulations, a square fabric of dimensions 200 mm × 200 mm is constrained at all the four edges.

Influence of surface mass density

Drape behaviour is related to the fabric surface mass density. In this section, we tested the sensibility of our deformable model implementation to this parameter. For this purpose, we simulated the response of the three fabrics with different surface mass densities. The results are illustrated in Figures 21 and 22. Mechanical and physical characteristics of fabrics F3-A and F3-B are same as those of fabric F3 except for surface masse densities, which are taken equal to 300 g m^{-2} and 400 g m^{-2}, respectively.

Fabric falling prediction

In this section, we illustrate fabric falling prediction using our deformable model implementation. In Figures 23 and 24, the falling of a rectangular fabric of

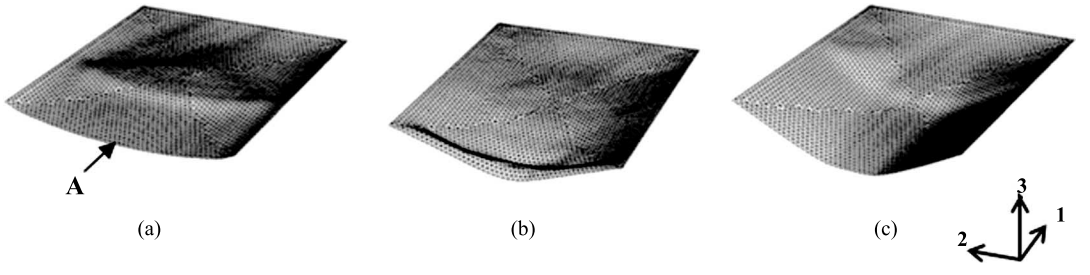

Figure 17. Influence of coefficients related to stretch–shear behaviour: (a) fabric F4, (b) fabric F4-A and (c) fabric F4-B.

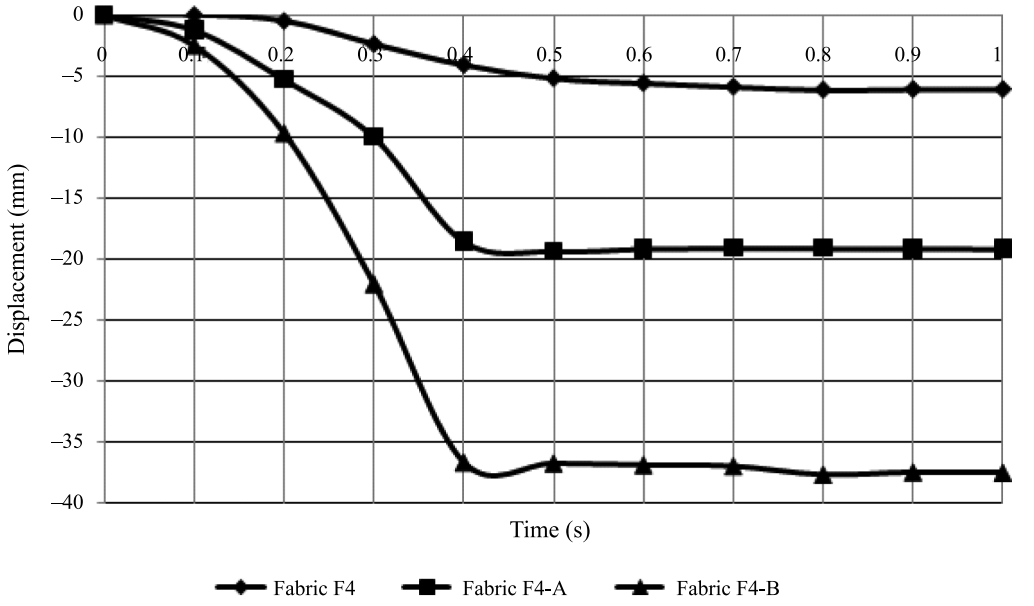

Figure 18. Displacement of the middle point of the free edge of fabrics F4, F4-A and F4-B.

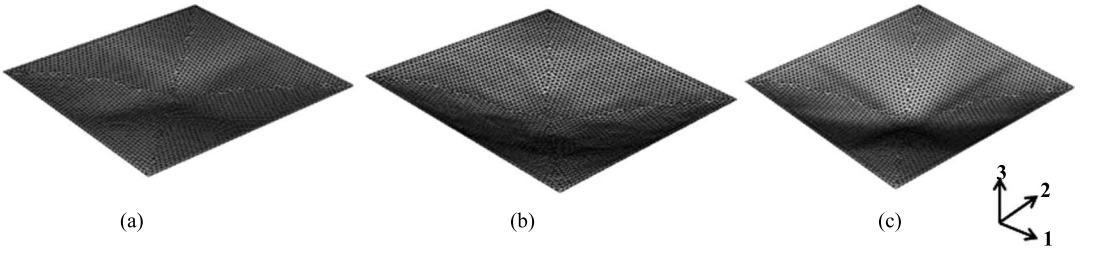

Figure 19. Influence of coefficients related to bending behaviour: (a) fabric F1, (b) fabric F1-A and (c) fabric F1-B.

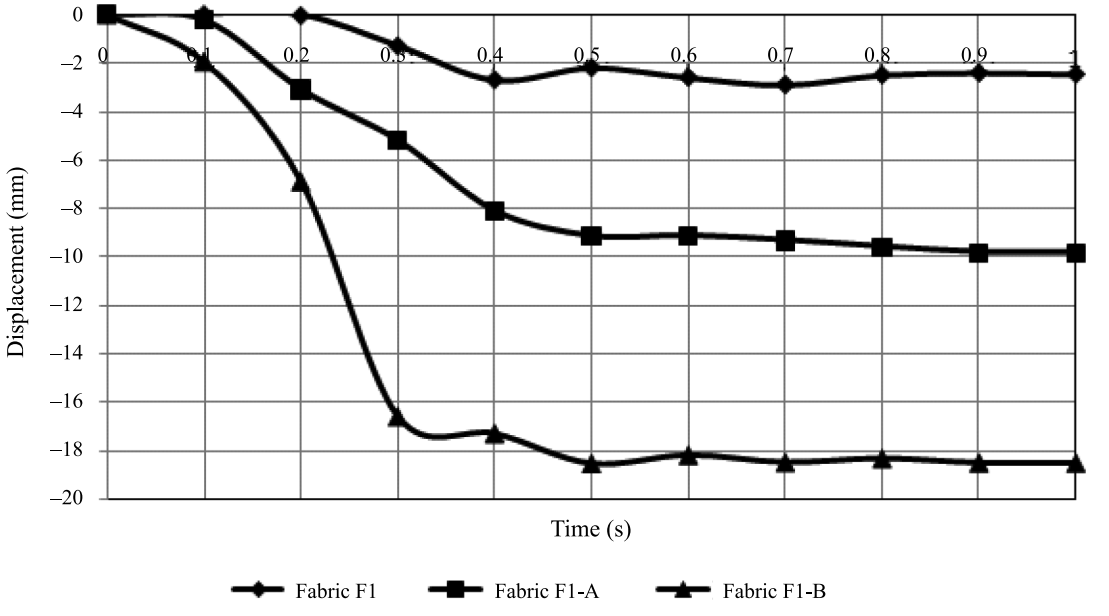

Figure 20. Displacement of the central point of fabrics F1, F1-A and F1-B.

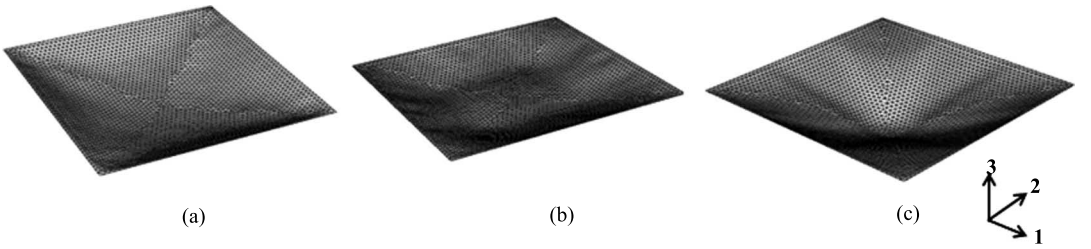

Figure 21. Influence of surface mass density: (a) fabric F3 (200 g m^{-2}), (b) fabric F3-A (300 g m^{-2}), and (c) fabric F3-B (400 g m^{-2}).

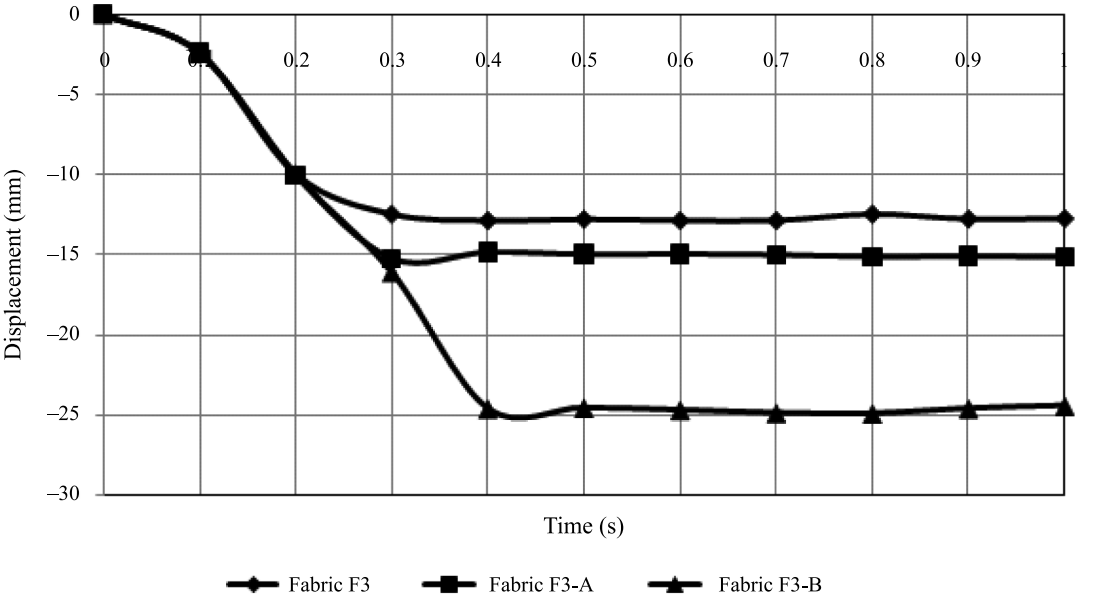

Figure 22. Displacement of the central point of fabrics F3, F3-A and F3-B.

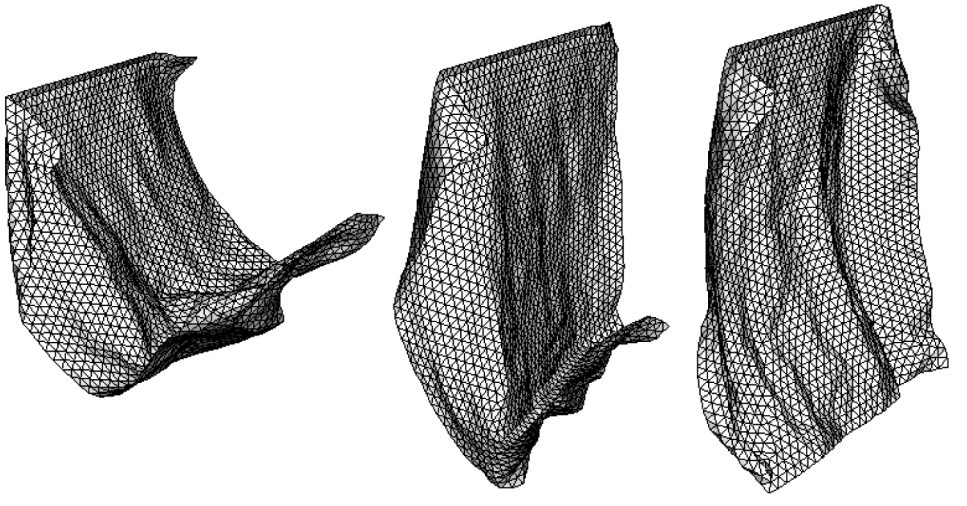

Figure 23. Fabric falling prediction (satin fabric F10).

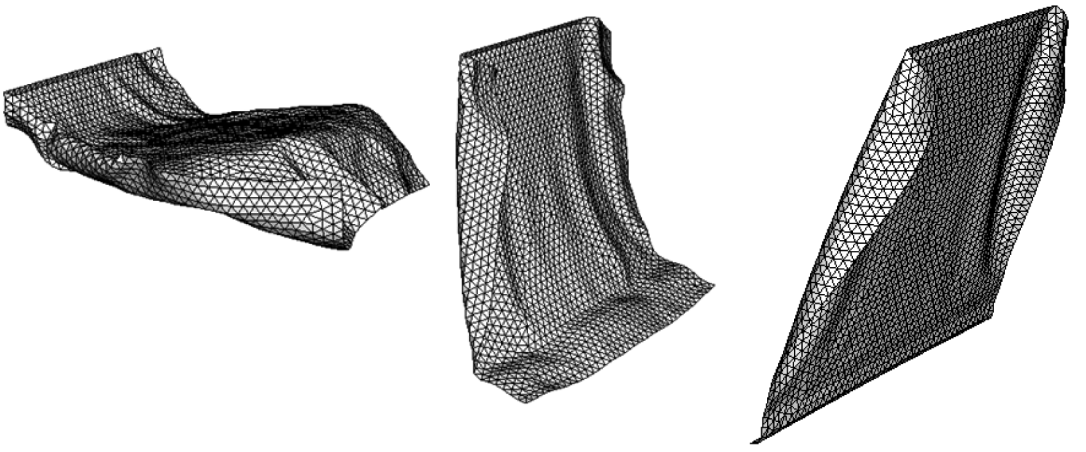

Figure 24. Fabric falling prediction (plain fabric F1).

dimensions 500 mm × 200 mm is presented. These fabrics are constrained at a part of the bottom edge and are subjected only to the action of their weight. Two types of fabrics are simulated: satin and twill fabrics. All these simulations are made using 7660 curvilinear triangular elements.

These simulations show the influence of the woven pattern as well as the influence of the mechanical coefficients of simulated fabrics on their fall. Indeed, the satin fabric F10, which is more flexible and elastic in comparison with the plain fabric F1, deforms to a greater degree and gives better configurations. This is in agreement with the real behaviour of satin fabrics.

Conclusion

In this paper, a formulation of deformable models is developed aiming at modelling and simulating the dynamic behaviour of textile fabrics. In this formulation, great importance is given to the physical and mechanical reality of woven fabrics. The parameters of the model are obtained by experimental characterization of 12 textile fabrics of varied textures. The resolution of the PDEs controlling the model is made by the FEM. A procedure of linearisation of these equations is developed.

As for the first investigation of this work, an apparatus (the drape-meter) usually used to characterize the deformability and drapeability of fabrics was simulated. The results obtained from the virtual drape-meter are in strong correlation with experimental measurements of the drape coefficient of various fabrics. However, for other characteristics of drape such as the number and dimensions of the nodes, the correlation is not strong enough between actual results and the virtual ones. This is explained by the fact that in simulation, we did not take into account the friction between fabric and the support disc, and the interactions (self-contact) between various nodes formed during simulations. Other simulations are also carried out by varying the configuration of the fabrics and by introducing other interactions, such as damping air flow. These simulations present fabrics draped on square tables or constrained at one of their points. Simulations of fabrics having various characteristics are carried out. The results obtained show the great sensitivity and capacity of our formulation to reproduce the changes in the texture of fabrics such as surface mass density, fabric pattern, rigidity to stretch–shear and bending behaviour.

This formulation remains of great utility to study other aspects of textile fabrics dynamics. Other more elaborated configurations can be simulated using this formulation. Moreover, we are planning to add the viscoelastic aspect of textile materials behaviour into this formulation.

References

Ascough, J., Bez, H., & Bricis, A. (1996). A simple beam element, large displacement model for the finite element simulation of cloth drape. *Journal of the Textile Institute, 87*(1), 152–165.

Baraff, D., & Witkin, A. (1998). Large steps in cloth simulation. In *SIGGRAPH 1998 Computer Graphics Proceedings, Annual Conference Series* (pp. 43–54). New York: ACM Press.

Behera, B.K., Pattanayak, A.K., & Mishra, R. (2008). Prediction of fabric drape using finite element method. *Journal of Textile Engineering, 54*(4), 103–110.

Bingham, G.A., Hague, R.J., Tuck, C.J., Long, A.C., Crookston, J.J., & Sherburn, M.N. (2007). Rapid manufactured textiles. *International Journal of Computer Integrated Manufacturing, 20*(1), 96–105.

Breen, D.E., House, D.H., & Getto, P.H. (1992). A physically-based particle model of woven cloth. *The Visual Computer, 8*(5–6), 264–277.

Breen, D.E., House, D.H., & Wozny, M.J. (1994). A particle-based model for simulating the draping behavior of woven cloth. *Textile Research Journal, 64*(11), 663–685.

Bridson, R., Fedkiw, R.P., & John, A. (2002). Robust treatment of collisions, contact, and friction for cloth animation. In *SIGGRAPH 2002 Conference Proceedings, Annual Conference Series* (pp. 594–603). New York: ACM Press.

Bruniaux, P., Ghith, A., & Vasseur, C. (2003). Modelling and parametric study of a fabric drape. *Advances in Complex Systems, 6*(4), 457–476.

Carignan, M., Yang, Y., Magnenat-Thalmann, N., & Thalmann, D. (1992). Dressing animated synthetic actors with complex deformable clothes. *Computer Graphics, 26*(2), 99–104.

Charlie, C.L., & Kai, T. (2008). Pattern computation for compression garment. In *SPM '08: Proceedings of the ACM Symposium on Solid and Physical Modeling* (pp. 203–211). Stony Brook, NY: ACM Press.

Chen, B., & Govindaraj, M. (1995). A physically based model of fabric drape using flexible shell theory. *Textile Research Journal, 65*(6), 324–330.

Chen, M., Sun, Q., & Yuen, M.-F. (1998). Simulation of fabric drape using thin plate element with finite rotation. *Acta Mechanica Sinica (English Series), 14*(3), 239–247.

Choi, K.-J., &, Ko, H.-S. (2005). Research problems in clothing simulation. *Computer-Aided Design, 37*, 585–592.

Ciarlet, P.G. (2005). *An introduction to differential geometry with applications to elasticity.* Dordrecht: Springer.

Collier, J.R., Collier, B.J., O'Toole, G., & Sarg, S. (1991). Drape prediction by means of finite-element analysis. *Journal of the Textile Institute, 82*(1), 96–107.

Cordier, F., Seo, H., & Magnenat-Thalmann, N. (2003). Made-to-measure technologies for an online clothing store. *IEEE Computer Graphics and Applications, 23*(1), 38–48.

De Santa, C.R., Wu, S.-T., & Costa, S.I. (1997). Analyzing a deformable model using differential geometry. In *Proceedings of the 10th Brazilian Symposium on Computer Graphics and Image Processing* (pp. 57–64). Compos do Jordao, Brazil: IEEE Computer Society.

Eberhardt, B., Olaf, E., & Michael, H. (2000). Implicit-explicit schemes for fast animation with particle systems. In N. Thalman-Magnenat, D. Thalman, & B. Arnaldi (Eds.), *Proceedings of the Eurographics Workshop on Computer Animation and Simulation (EGCAS-00)* (pp. 137–151). Wien, Austria: Springer-Verlag.

Fontana, M., Carubelli, A., Rizzi, C., & Cugini, U. (2005). Cloth assembler: A CAD module for feature-based garment pattern assembly. *Computer-Aided Design & Applications, 2*(6), 795–804.

Fontana, M., Rizzi, C., & Cugini, U. (2004). Physics-based modelling and simulation of functional cloth for virtual prototyping applications. In *SM '04: Proceedings of the 9th ACM symposium on Solid Modeling and Applications* (pp. 267–272). Aire-la-Ville, Switzerland: Eurographics Association.

Garg, A., Grinspun, E., Wardetzky, M., & Zorin, D. (2007). Cubic shells. In *SCA '07: Proceedings of the 2007 ACM SIGGRAPH/Eurographics symposium on Computer Animation* (pp. 91–98). Aire-la-Ville, Switzerland: Eurographics Association.

Goldstein, H., Poole, C., & Safko, J. (2000). Classical mechanics (3rd ed.). San Francisco, CA: Addison Wesley.

Hauth, M., Etzmuß, O., & Straßer, W. (2003). Analysis of numerical methods for the simulation of deformable models. *The Visual Computer, 19*(7–8), 581–600.

Hauth, M., Etzmuss, O., Eberhardt, B., Klein, R., Sarlette, R., Sattler, M., Danbert, K., Kautz, J. (2002, September). *Cloth animation and rendering*. Paper presented at the 23rd Annual Conference of The European Association for Computer Graphics, The Eurographics Association, Saarbrücken, Germany.

In, H.S., Tae, J.K., Sung, M.K., & Chi, Y.-S. (2006). Simulation of cusick drapemeter using particle-based modeling: Stability analysis of explicit integration methods. *Textile Research Journal, 76*(9), 712–719.

Jeffrey, E., Shigan, D., & Timothy, G.C. (1996). Finite element modeling and control of flexible fabric parts. *IEEE Computer Graphics and Applications, 16*(5), 71–80.

Kang, T.J., & Yu, W.R. (1995). Drape simulation of woven fabric by using the finite-element method. *Journal of the Textile Institute, 86*(4), 635–648.

Kim, M.S., & Kang, J. (2002). Garment pattern generation from body scan data. *Computer-Aided Design, 35*, 611–618.

Kravchuk, A.S., & Neittaanmäki, P.J. (2007). *Variational and quasi-variational inequalities in mechanics.* Dordrecht: Springer.

Liang, M., Jinlian, H., & Baciu, G. (2006). Generating seams and wrinkles for virtual clothing. In *VRCIA '06: Proceedings of the 2006 ACM International Conference on Virtual Reality Continuum and Its Applications* (pp. 205–211). Hong Kong, China: ACM Press.

Liu, X.H., & Sze, K.Y. (2009). A corotational interpolatory model for fabric drape simulation. *International Journal for Numerical Methods in Engineering, 77*, 799–823.

Luo, Z.G., & Yuen, M.M. (2005). Reactive 2D/3D garment pattern design modification. *Computer-Aided Design, 37*, 623–630.

Magnenat-Thalmann, N., Volino, P., & Cordier, F. (2002). Avenues of research in dynamic clothing. In *Proceedings of the Computer Animation 2002.* Washington, DC: IEEE Computer Society.

Manuel, D.L., & Paulo R.R. (1989). *Methods of differential geometry in analytical mechanics.* Amsterdam: Elsevier Science B.V.

Müller, M., Heidelberger, B., Hennix, M., & Ratcliff, J. (2007). Position based dynamics. *Journal of Visual Communication and Image Representation, 18*, 109–118.

Oh, S., Noh, J., & Wohn, K. (2008). A physically faithful multigrid method for fast cloth simulation. *Computer Animation and Virtual Worlds, 19*, 479–492.

Palmer, P., Mir, A., & González, M. (2000). Stability and complexity study of animated elastically deformable objects. In H.H. Nagel & F.J. Perales (Eds.), *Articulated motion and deformable object* (pp. 58–71). Berlin/Heidelberg: Springer-Verlag.

Provot, X. (1995). Deformation constraints in a mass-spring model to describe rigid cloth behavior. In *Proceedings of Graphics Interface '95* (pp. 147–154). Québec, Canada: AK Peters.

Saville, B.P. (1999). *Physical testing of textiles.* Cambridge: Woodhead Publishing.

Stylios, G.K., Wan, T.R., & Powell, N.J. (1996). Modelling the dynamic drape of garment son synthetic humans in a virtual fashion show. *International Journal of Clothing Science and Technology, 8*(3), 95–112.

Terzopoulos, D., & Fleischer, K. (1988a). Modeling inelastic deformation: Viscoelasticity, plasticity, fracture. *Computer Graphics, 22*(4), 269–278.

Terzopoulos, D., & Fleischer, K. (1988b). Deformable models. *The Visual Computer, 4*, 306–331.

Terzopoulos, D., Platt, J., Barr, A., & Fleischer, K. (1987). Elastically deformable models. *Computer Graphics, 21*(4), 205–214.

Terzopoulos, D., & Witkin, A. (1988). Physically based models with rigid and deformable components. *Computer Graphics and Applications, 8*(6), 41–51.

Volino, P., Cordier, F., & Magnenat-Thalmann, N. (2005). From early virtual garment simulation to interactive fashion design. *Computer-Aided Design, 37*, 593–608.

Volino, P., & Magnenat-Thalmann, N. (2001). Comparing efficiency of integration methods for cloth simulation. In *CGI '01: Proceedings of International Computer Graphics* (pp. 265–272). Washington, DC: IEEE Computer Society.

Volino, P., & Magnenat-Thalmann, N. (2005). Accurate garment prototyping and simulation. *Computer-Aided Design & Applications, 2*(5), 645–654.

Wu, S.-T., & de Melo, V.F. (2004). A deformable surface model on the basis of the theory of a Cosserat surface. In *Sibgrapi 2004: Proceedings of 17th Brazilian Symposium on Computer Graphics and Image Processing* (pp. 274–281). Curitiba, Brazil: IEEE Computer Society.

Yu, W.R., Kang, T.J., & Chung, K. (2000). Drape simulation of woven fabrics by using explicit dynamic analysis. *Journal of the Textile Institute, 91*(2), 285–301.

Yu, W.R., Zampaloni, M., Pourboghrat, F., Chung, K., & Kang T.J. (2005). Analysis of flexible bending behavior of woven preform using non-orthogonal constitutive equation. *Composites Part A, 36*(6), 839–850.

Zink, N., & Hardy, A. (2007). Cloth simulation and collision detection using geometry images. In *AFRIGRAPH '07: Proceedings of the 5th international conference on Computer Graphics, Virtual Reality, Visualisation and Interaction in Africa* (pp. 187–195). Grahamstown, South Africa: ACM Press.